INFLUENCE OF DEFORMATION ON THE INTERFACE PROPERTIES OF COATED FUSELAGE SHELLS

[1]Jan JEPKENS, [1]Norman MOHNFELD, [1]Philipp MÜLLER, [1]Hendrik WESTER, [1]Sven HÜBNER, [2]Simon WEHRMANN, [1]Bernd-Arno BEHRENS

[1]IFUM – Leibniz University Hannover, Hannover, Germany, EU, jepkens@ifum.uni-hannover.de, mohnfeld@ifum.uni-hannover.de, wester@ifum.uni-hannover.de, mueller@ifum.uni-hannover.de, huebner@ifum.uni-hannover.de, behrens@ifum.uni-hannover.de

[2]Deharde GmbH, Varel, Germany, EU, s.wehrmann@deharde.de

https://doi.org/10.37904/metal.2024.4892

Abstract

Aircraft fuselage shells made from aluminium are coated to withstand the external influences from aviation. The corrosion protection consists mainly of an anodic oxide layer as the interface (IF) and a primer as the coating. As the coating can be damaged during the forming process, Original Equipment Manufacturers (OEMs) such as Airbus restrict the process chain so that the coating may only be applied onto the finished formed part. Previous studies with regard to the evolution of coating properties during forming have shown that a particular incremental bending process known as Deharde Polygon Forming® (DPF®) shows the potential to overcome these limitations. Thus, it could be possible to apply coatings to flat sheets before forming. That could save energy as well as environmentally harmful alkalis and acids for anodizing. As the IF shows the highest hardness of the coating-interface-substrate (CIS) system combined with a small thickness, it can be assumed that the IF is more endangered to failure. This paper therefore presents the results of an analysis of the interface before and after forming. Scaled fuselage shells are incrementally bent by DPF® to induce process-related deformations. Specimens from the initial state and from scaled fuselage shells are investigated by scratch and indentation tests with a Triboindenter TI 950. Due to the low plastic deformations induced by incremental bending with DPF® neither Young's modulus and hardness nor elastic and plastic behaviour undergo significant changes. Hence the obtained results imply opportunities for flexible adjustments to the process chain regarding forming and coating.

Keywords: Incremental bending, fuselage shells, interface properties, coating, nanoindentation, scratch, SPM

1. INTRODUCTION

Aluminium is the most commonly used material for aircraft fuselage shells due to its combination of high specific strength and formability [1]. The aluminium-copper alloy EN AW-2024, favoured for fuselage shells, is susceptible to corrosion and hydrogen embrittlement [2]. To ensure corrosion protection under aviation conditions, fuselage components can be anodised and coated with an organic epoxy-based primer [3]. A requirement of the corrosion protection is its integrity and stability during service life in aviation [4]. Accordingly, OEMs such as Airbus have strict specifications for the coating. These mandatory process instructions include the requirement that forming must be performed prior to anodising and coating [5]. Evolutionary, the specifications were driven by stresses and strains induced by forming processes such as roll and stretch forming, which can lead to coating failure. Roll forming is mainly applied for the production of fuselage shells with cylindrical radii [6]. During this process, a superimposed stress state with considerable shear stresses is induced by relative movement of the tool and sheet metal [7], which causes the risk for failure. Stretch forming is used to manufacture fuselage shells with cylindrical and additional curvature in the longitudinal direction,

also referred to as spherical shells [8]. In this context, previous analyses of pre-deformed Marciniak specimens in the stretch forming stress state have already shown a failure of the primer for an elongation of 0.025. According to the previous study, it is evident that an incremental bending process, known as Deharde Polygon Forming® (DPF®), avoids failure of the primer coating during forming by inducing lower strains and compressive stresses close to the surface. Following up on the previous analysis, this paper investigates the suitability of the DPF® for the forming of coated fuselage shells focusing on the anodised interface. The investigation is motivated by the potential saving of a significant amount of environmentally harmful alkalis and acids, which is possible by adjusting the process chain and anodising plane sheets prior to forming.

2. MATERIALS AND METHODS

In order to assess the suitability of the DPF® for the forming of coated fuselage shells, specimens were compared in the initial state and after forming by nanoindentation and scratch tests. Subject of the investigation was the aluminium-copper alloy EN AW-2024-T351 with an epoxy-based coating of Seevenax-313-81 primer. The resulting CIS system is common for aircraft fuselage components. However, the focus of this analysis was on the interface between aluminium and the coating. As the interface has the highest hardness and smallest thickness in the CIS system, it is most susceptible to failure. Deformations were induced by the scaled DPF® tool shown in **Figure 1 (a)**. The entire setup was mounted in a Dunkes HDZ 400 hydraulic double column press.

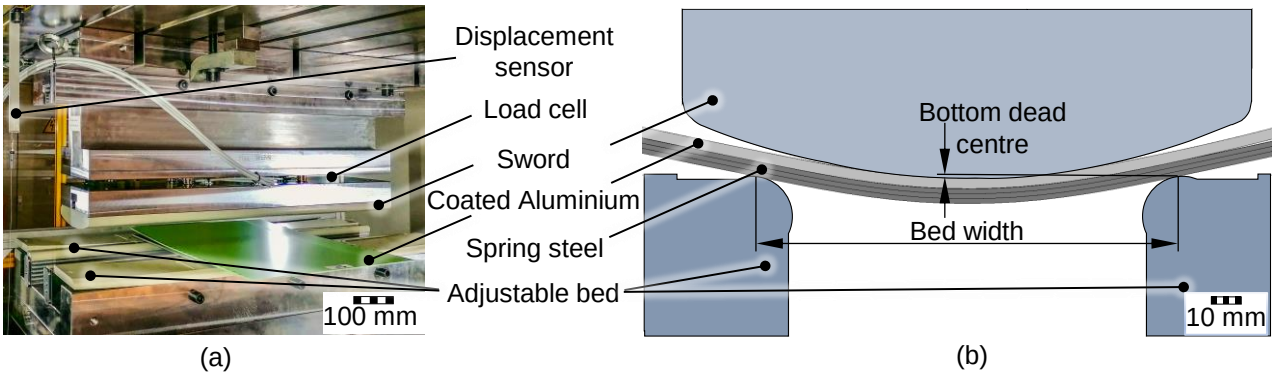

Figure 1 (a) Scaled DPF® tool; (b) Scheme of DPF® tool and process parameters in side view

Three scaled fuselage shells were formed from which specimens were obtained. The initial dimensions of the aluminium workpiece were 500 x 500 x 3.36 mm³. For the incremental bending process, the aluminium was positioned on three spring steel sheets made of 1.1274. The rolling directions of the steel sheets and the aluminium workpiece were parallel to the sword length. Each spring steel sheet measured 500 x 300 x 1.5 mm³. **Figure 1 (b)** shows that the spring steel sheets were placed on the bed as additional plane support. This also allows the edge areas to be formed. The radius of the roller bed was 12 mm and the bed width was 132 mm. The strokes were performed displacement-controlled by a sword with a radius of 215 mm up to a bottom dead centre of -0.8 mm at a velocity of 10 mm/s. In total, the incremental bending process consists of 24 strokes with a distance of 20 mm. For each stroke, the workpiece was manually positioned using corresponding marks for the position of the spring steels on the bed. The workpiece is positioned relative to the midline of the centred spring steels by means of corresponding markings every 20 mm for each stroke.

Standard fuselage shells have radii between 1800 mm and 2600 mm. For a conservative assessment of the suitability of DPF® to form coated fuselage shells, scaled fuselage shells with smaller inner radii were manufactured using the specified parameters. As the induced strains are too small for a valid optical measurement, the formed state is characterised by the inner radius. For this purpose, the geometry of the scaled fuselage shells was measured optically using an ATOS 2 400 system from Carl Zeiss GOM Metrology

GmbH. To calculate the inner radii, the local coordinates of the cross-sections were exported on the centre line and ±100 and ±200 mm from the centre line, as depicted in **Figure 2 (a)**. Using the exported coordinates, the inner radii were calculated and averaged according to the approach in **Figure 2 (b)**. Thus, the inner radius of three scaled fuselage shells with five cross-sections each was 1163.5 mm on average, as shown in **Figure 2 (c)**.

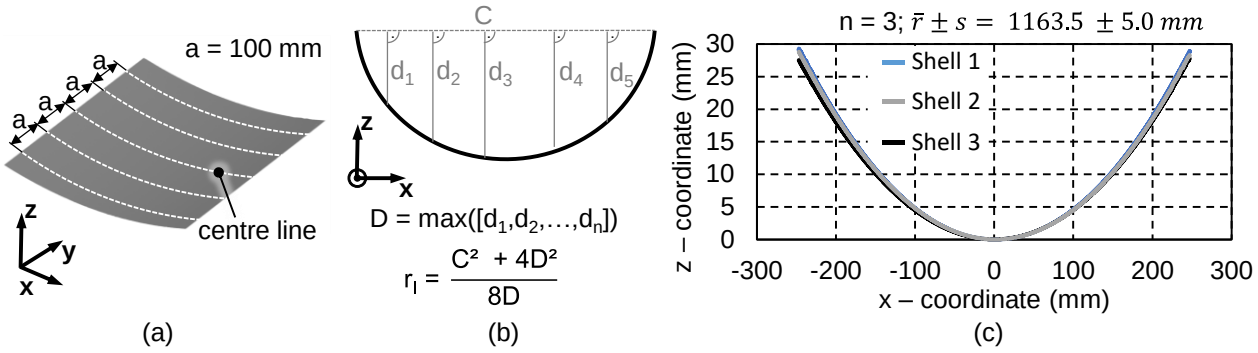

Figure 2 (a) Position of cross-sections; (b) Calculation of inner radii; (c) Final inner radii at centre line

In order to correlate the deformation of the interface with the final results of the nanoindentation and scratch test, the strain state is calculated using finite element (FE) models. Therefore, FE models for the incremental forming of uncoated fuselage shells, developed in the corresponding project, were used. The details of the material modelling, the FE models, the calculation with LS-Dyna and the validation follow the approach of Jepkens et al. [9]. The corresponding strain distribution of the examination area after the entire incremental process is shown in **Figure 3 (a)**. The surface is compressed on the inside and stretched on the outside. **Figure 3 (b)** specifies the quantitative evolution of the strain over the sheet thickness. The inner side is compressed by -0.8% during forming of the 12th stroke. After springback and release of elastic strains, a small residual plastic strain of about -0.16% remains. As the incremental process continues, the area of the 12th stroke is partially loaded again and additional residual tensile stresses are left on the inside after springback. Thus, at the end of the entire incremental process, the residual stresses in the examination area are reduced to approximately -0.14% on the inside. Equivalent and opposite effects can be observed on the outside.

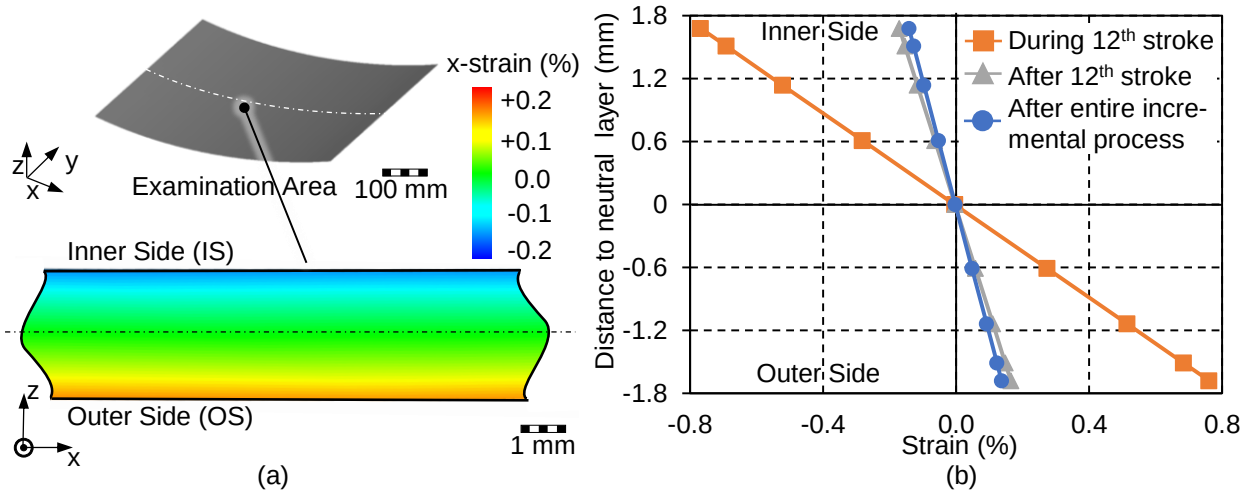

Figure 3 (a) Through-thickness strain distribution of examinaton area after entire incremental process; (b) Evolution of through-thickness strain distribution

Three formed and three initial specimens were water jet cut to a size of 5 x 5 mm², cold embedded, grinded and polished to investigate the mechanical and tribological properties. Analysis was carried out on a TI950 triboindenter from Hysitron at the initial state and on both the inner and outer sides of the formed specimen. The cross-section was screened with indents using a Berkovich diamond tip with a tip radius of 100 nm. Hence, nano hardness and Young's modulus were determined at a spacing of 2 µm for the coating as well as aluminium and 0.8 µm for the interface for a cross-section of 220 x 40 µm². The load was applied with a trapezoidal function up to a maximum test load of 250 µN for the coating, 2000 µN for the interface and 350 µN for the aluminium. A conical diamond tip with a radius of 300 nm was used to characterise the elastic and plastic properties of the interface. Nine scratch tests, consisting of pre-scan, scratch and post-scan, were performed for each variant. In these tests, the normal force was linearly raised from 2 µN to 500 µN over an 8 µm scratch length. The scratch test follows the method described in detail by Pape and Gatzen [10]. In order to assign the nano hardness mappings to the individual layers of the CIS-system, the microstructure of the specimens was analysed after polishing and etching with Barker's method. Images in the initial state were taken with a light microscope Polyvat Met from Reichert and Jung.

3. RESULTS

Figure 4 correlates the microstructure in the initial state and the nano hardness mapping before and after forming. It is evident that the epoxy-based primer shows the lowest nano hardness with values below 0.875 GPa. The base metal EN AW-2024-T351 has a basic hardness of around 2.625 GPa. Towards the surface, the nano hardness of the aluminium alloy decreases to a level of 1.75 GPa. This is caused by the formation of coarse grains near the surface. The interface between the primer and the aluminium has the highest nano hardness at approximately 6.125 GPa. After forming, the distribution and level of the nano hardness mapping is consistent.

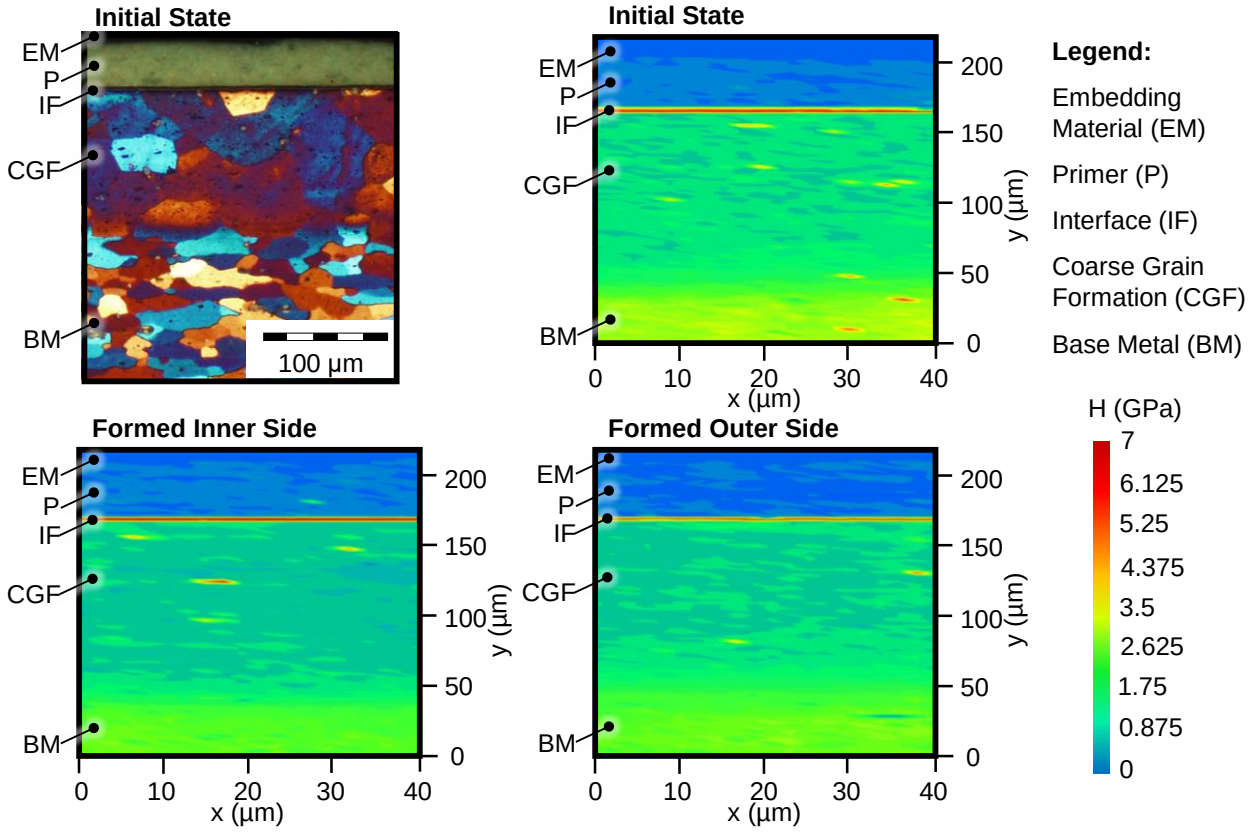

Figure 4 Microstructure and nano hardness mapping of the CIS system in the initial state and after forming

Due to the low layer thickness and the highest nano hardness of the interface, it is prone to failure. Therefore, nano hardness and Young's modulus are quantified in detail in **Figure 5** using boxplots. In the initial state, the median nano hardness is 5.5 GPa. As a result of forming, nano hardness on the inside increases by around 7.5% to nearly 6 GPa, while the values on the outside remain at the same level as before forming. In addition, the interquartile distances represented by the coloured and striped boxes are 0.34 GPa in the initial state, 0.51 GPa on the inside and 0.9 GPa on the outside in the formed state. Accordingly, 50% of the measured data lies directly around the median. Combined with the nano hardness maps from **Figure 4** and the maximum and minimum values of the box plot from **Figure 5**, no critical local loss of nano hardness could be detected. The results for Young's Modulus are consistent. The median before and after forming is at a constant level between 82 and 84 GPa. Neither the extreme values nor the interquartile ranges with values between 10 and 12 GPa indicate any critical local inhomogeneities.

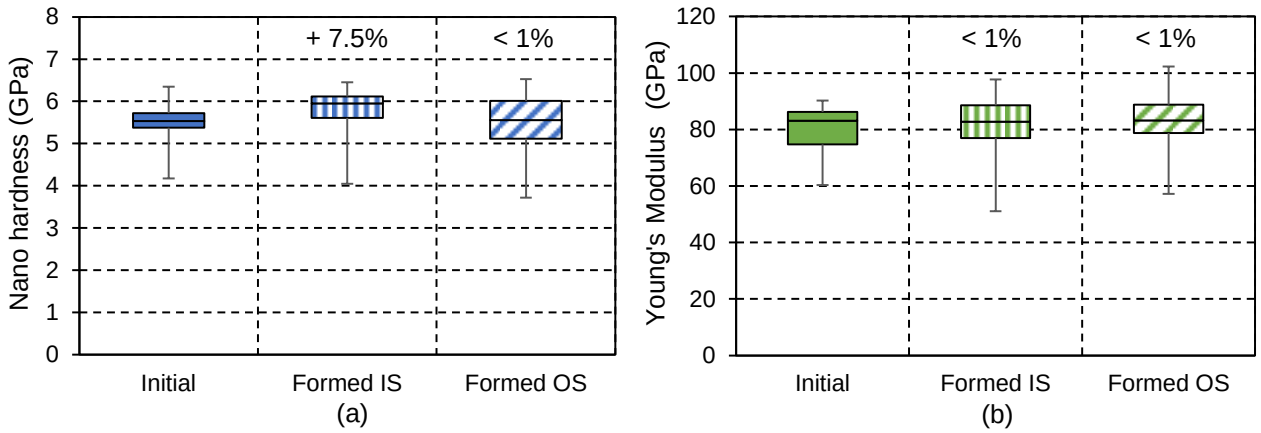

Figure 5 Boxplots of (a) Nano hardness and (b) Young's modulus before and after forming

Moreover, **Figure 6 (a)** summarises the results of the scratch tests. The elastic compared to the plastic behaviour shows a ratio of 0.46 to 0.54. After forming, the interface behaves more plastically on the inner side, which is shown by an increase of 10%. Overall, the ratio of elasticity and plasticity shifted towards 0.41 to 0.59. A reverse change was observed on the outer side. Here, the elastic portion increases by 22% while the plastic ratio decreases by 16%. Thus, a ratio of 0.5 to 0.5 was found. **Figure 6 (b)** contains the results of the stress distribution over the sheet thickness in the examination area, obtained from the simulation of the DPF®.

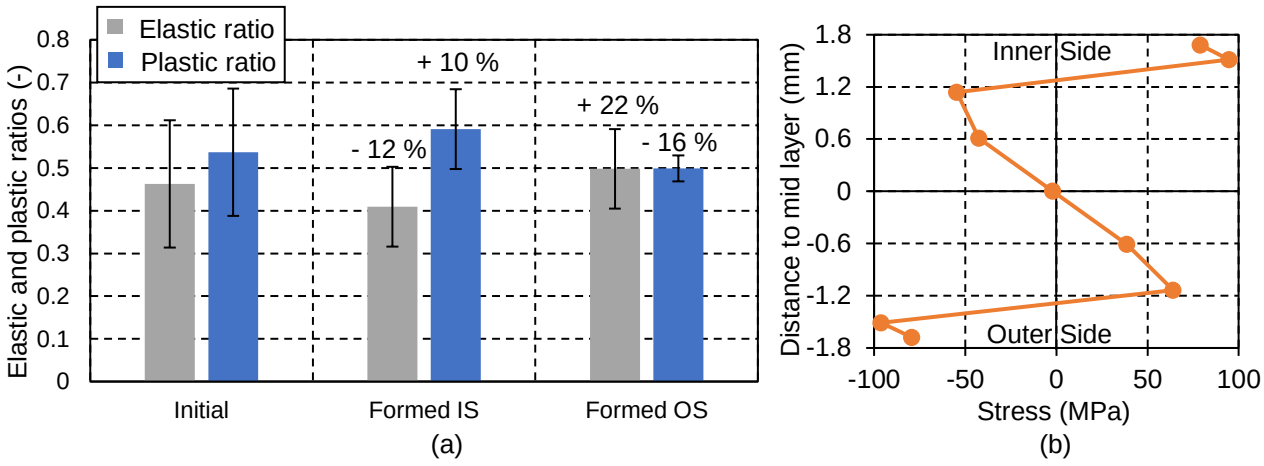

Figure 6 (a) Elastic and plastic interface behaviour before and after forming;
(b) Simulated through-thickness residual stress distribution of examination area

Correlating the stress distribution with the elastic-plastic interface behaviour implies the following relation for the outer side. On the one hand, the existing residual compressive stresses hinder the indentation of the conical diamond tip for the scratch test, which reduces the plastic deformation. On the other hand, the resetting effect of the residual compressive stresses leads to higher springback after the test, which results in a relative increase in elasticity. Considering standard deviations ranging from 16 to 32%, it is advisable not to overemphasize the observed changes of 10 to 22%.

4. CONCLUSION AND OUTLOOK

In terms of interface analysis, neither hardness nor Young's modulus showed any adverse changes. Local inhomogeneities could be excluded by contextualisation of box plots and hardness mappings. Furthermore, the changes in elastic and plastic behaviour in the scratch test are within the standard deviation. One reason for the minor changes are the remaining strains after DPF®, which are below 0.15%. Accordingly, the results indicate the suitability of DPF® for forming of coated fuselage shells. Accordingly, coating could be performed before forming, which would save energy and environmentally harmful alkalis and acids. Since incremental bending by DPF® relies on peripheral processes such as handling, further investigations should focus on assessing the influence of handling on the integrity of the coating. Additionally, appropriate corrosion tests should be conducted.

ACKNOWLEDGEMENTS

The paper was obtained within the project "Aggregated Polygon Forming based Processes for large Fuselage Components" (ZW1-80159743), funded by the Investitions- und Förderbank Niedersachsen – NBank. The authors gratefully acknowledge NBank for their financial support.

REFERENCES

[1] LI, S.-S., YUE, X., LI, Q.-Y.; PENG, H.-L., DONG, B.-X., LIU, T.-S., YANG, H.-Y., FAN, J., SHU, S.-L.; QIU, F., JIANG Q.-C. Development and applications of aluminum alloys for aerospace industry. *Journal of Materials Research and Technology* 2023, vol. 27, pp. 944–983.

[2] PANTELAKIS, S.G., PETROYIANNIS, P.V., KERMANIDIS, A.T. Corrosion and Hydrogen Embrittlement of the the 2024 Aircraft Aluminum Alloy. *Corrosion Reviews* 2007, vol. 25, pp. 363–376.

[3] JOTHI, V., AADESINA, A.Y., KUMAR, A.M., AL-AQEELI, N., RAM, J.N. Influence of an anodized layer on the adhesion and surface protective performance of organic coatings on AA2024 aerospace Al alloy. *Progress in Organic Coatings* 2020, vol. 138.

[4] PAZ MARTINEZ-VIADEMONTE, M., ABRHAMI, S.T., HACK, T., BURCHARDT, M. TERRYN, H. A Review on Anodizing of Aerospace Aluminum Alloys for Corrosion Protection. *Coatings.* 2020, vol. 10, pp. 1106-1135.

[5] AIPI02-01-003. *AIPI Airbus Process Instruction: Tartaric Sulphuric Anodizing of aluminum alloys for corrosion protection and paint pre-treatment.* AIRBUS Operations S.A.S., 2020.

[6] PENG, J., LI, W., WAN, M., ZHANG, C., LI, J., SUN, G. Investigation on three-roller cylindrical bending of 2060-T8 Al-Li alloy plate for aircraft fuselage skin components. *International Journal of Material Forming* 2018, vol.*11*, pp. 269–278.

[7] PANTON, S.M., DUNCAN, J.L., ZHU, S.D. Longitudinal and shear strain development in cold roll forming. *Journal of Materials Processing Technology.* 1996, vol. 60, pp. 219–224.

[8] PENG, J., LI, W., HAN, J., WAN, M., MENG, B. Kinetic locus design for longitudinal stretch forming of aircraft skin components. *International Journal of Advanced Manufacturing Technol*ogy. 2016, vol. *86*, pp. 3571–3582.

[9] JEPKENS, J., MÜLLER, P., WESTER, H., HÜBNER, S., WEHRMANN, S., BEHRENS, B.-A. Simulation and Validation of an Incremental Bending Process for Cylindrical Fuselage Components. *Aerospace* 2024, vol. 11.

[10] PAPE, F., GATZEN, H. Tribological Behavior of Multilayer Diamond-like Carbon (DLC) Coatings. In: *Reibung, Schmierung und Verschleiß.* Aachen: GfT, 2008.